Effects of flame retardants on extinction limits, spread rate, and smoke release in opposed-flow flame spread over thin cylindrical polyethylene samples in microgravity

Y. Li[a,*], A. Guibaud[b], J.-M. Citerne[a], J.-L. Consalvi[c], A. Coimbra[c]
J. Sarazin[d], S. Bourbigot[d,e], J.L. Torero[b], G. Legros[a]

[a] *Institut Jean Le Rond d'Alembert/UMR CNRS 7190, Sorbonne Université, Paris F-75005, France*
[b] *Department of Civil, Environmental and Geomatic Engineering, University College London, London WC1E6BT, UK*
[c] *Aix-Marseille Université, CNRS, IUSTI UMR 7343, 5 rue E. Fermi, 13013 Marseille, France*
[d] *Université de Lille, CNRS, INRAE, Centrale Lille, UMR 8207 – Unité Matériaux et Transformations, F-59000, Lille, France*
[e] *Institut Universitaire de France (IUF), Paris, France*

Abstract

Though flame retardants are considered for use in spacecraft, their performances in microgravity are still poorly understood. To assess their effects on flame extinction, opposed flame spread rate, and smoke emission in the absence of buoyant flows, thin cylindrical samples of Low Density Polyethylene (LDPE) loaded with intumescent flame retardants are ignited in parabolic flights. Two types of flame retardants characterized by different mechanisms of intumescence are considered, namely Expandable Graphite, (EG), and Ammonium polyphosphate / Pentaerythritol, (AP), for which thermal stress and chemical recombination drive physical expansion, respectively. Observations are then reported and contrasted with results obtained at normal gravity for different flame retardant loads, under varying oxygen content at given ambient pressure and flow velocity. Focusing on the flame leading edge, results related to flame spread and flame extinction are analyzed first. At normal gravity, increasing the flame retardant load improves fire safety through an increase in the flame extinction limit on the one hand, and a reduction in the average flame spread rate for all oxygen contents studied on the other hand. In contrast, results in microgravity show no modification in the extinction limit over the range of flame retardant loads studied, and the benefits in average flame spread rate reduction are less pronounced. Investigating then radiative quenching at the flame trailing edge, smoke emission is never evidenced at normal gravity. However, in microgravity, the addition of flame retardants increases the range of conditions leading to smoke emission, which is detrimental to fire safety. These observations are valid for both flame retardants, yet more pronounced for EG-loaded samples than AP-loaded samples. These ambivalent effects on fire safety of AP and EG addition in microgravity, which are not evidenced at normal gravity, call for a cautious integration of flame retardants in the scope of space exploration.

Keywords: Flame retardant; Microgravity; Flame spread; Extinction limits; Smoke emission

1. Introduction

Fire safety has been identified as one of the most important issues that must be properly resolved in manned spaceflight [1], since an accidental fire can jeopardize the missions and even pose a threat to the health and life safety of astronauts in the worst-case scenarios. With the increase in both distance and duration of space travel in the context of lunar habitats development or deep space exploration ambitions, fire safety issues are twofold. From a technological perspective, the existing fire strategies designed for low earth orbit spacecraft rely on the possibility to conduct fast resupply missions after minor fire incidents, or to perform short-range emergency evacuations if the situation deteriorates. Unfortunately, both options are not accessible beyond Earth's orbit. From a fundamental perspective, the dramatic impact of reduced gravity on material flammability, ignition conditions, flame spread, fire growth, and smoke emission through modifications in heat and mass transfer is still not fully understood and remains an active topic of academic research [2, 3]. Thus, to develop relevant fire strategies in the absence of buoyancy, these fire safety aspects are being studied over a range of materials, e.g. composite cotton fabric [4], PMMA [5], and polyethylene [6], and over geometries such as flat sheets [7] and cylinders [8] to create a comprehensive base of knowledge for further investigations. Cylindrical Low-Density PolyEthylene (LDPE) is one of the most studied configurations, and can thus be used as a baseline material to expand our knowledge in this field. It has been found that the probability of ignition of LDPE is significantly increased in microgravity conditions as compared with a standard gravity level [9]. In addition, as buoyant flows disappear, a flame can spread over these samples under low oxygen content conditions that would lead to flame self-extinction at normal gravity [10]. Moreover, more intense smoke production is reported in the absence of buoyancy [11] owing to increased radiative losses from sootier flames [12], which is consistent with observations from a major past incident aboard the Mir Space Station [13]. All these observations suggest an increased danger in the confined environment of a spacecraft.

Though leading aspects of combustion are modified in microgravity, the associated fire safety concerns are not specific to space exploration. As such, inspiration can be found in existing solutions from other industries. For instance, flame resistant or flame retardant materials are commonly employed in construction, transport, cable, or textile industries to improve fire safety, and should be considered in spacecraft design as well. Flame resistant fabrics are made from materials that inherently have low flammability properties, while flame retardant fabrics have been modified by chemical coating or inclusion and thermal treatments to improve on their original behavior.

Concerning flame resistant materials, Orndoff summarized the successful development of several fabrics for space exploration by textile industries since the 1960s, like polybenzimidazole fibers, aromatic polyamide fibers, chlorofluoroethylene fibers, polyimide fibers, and beta fiberglass [14]. These materials could eventually pass flammability tests on the ground to assess their viability in an oxygen-enriched atmosphere (beta fiberglass for instance was designed to be non-flammable in the pure oxygen environment of a spacesuit), and were included in the design of successive spacecraft. However, the tests were not performed in the absence of buoyancy, so it is not known whether these flame retardant fabrics perform in microgravity as well as they do at normal gravity. In addition, their prohibitive cost and limited range of applications hampers a sustainable production. Investigating the difference caused by buoyancy, Takahashi et al. compared flammability of other more common flame resistant materials, such as NOMEX, Kevlar, Kapton, CARBOGLASS, PEEK, PPSU, silicone resin, and silicone rubber, under both normal and micro-gravity [15, 16]. They found that, among these materials, those with higher pyrolysis temperatures inhibit flame spread in microgravity and can self-extinguish under higher oxygen content than observed at normal gravity. Because they are inherently designed for specific fire needs, flame resistant materials may poorly address other functional requirements vital to space travel [14].

As such, research on flame retardant materials has also received a special focus to boost the fire properties of existing materials used in spacecraft at a limited development cost. To protect spacecraft and astronauts following the catastrophic 1967 Apollo 1 fire, Parker et al. [17] considered enhancing the fire resistance properties of polymeric materials by adding flame retardant coatings (nitroanailine-sulfonic acids, quinonedioxime-acid mixtures, and nitroanilinosulfones). The nitroanailine-sulfonic acids coating had been tested for its effectiveness in protecting a structure from the fire on the ground and it was shown that the temperature of the coated sample increased five times slower than in the absence of coating. With the same purpose, Kourtides et al. [18] conducted experiments on composite materials loaded with flame retardants (graphite-reinforced composites) on the ground. They found that the loaded samples showed a higher limiting oxygen index (LOI), lower heat release rate, and lower smoke production. These two reports aside, there is a lack of measurements regarding the efficiency of flame retardants in the context of space exploration, amplified by the absence of data in reduced gravity.

In this context, a broad range of flame retardants can be investigated. Intumescent flame retardants, which expand when exposed to external heating while retaining acceptable mechanical properties, are especially relevant in polymer materials increasingly used in spacecraft. In the presence of a flame, an expanded char layer can be formed, inhibiting fire spread by slowing down heat and mass transfer between the gas and condensed phases [19]. Intumescence can

be obtained from a series of chemical reactions or using mechanical expansion. Ammonium polyphosphate/pentaerythritol (AP) is a system consisting of ammonium polyphosphate (APP) and PentaERythritol (PER), producing intumescence via a series of chemical reactions. Under the action of external heat flux, APP decomposes and yields acidic phosphates acting as char promoters. Phosphates react with PER to yield char which can expand to a porous char layer, thanks to the evolution of ammonia from APP and the decomposition products of the burning material [20]. Therefore, the post-combustion AP residue is an expanded carbonaceous char, acting as a heat barrier. Its internal structure is foamy with small and large voids. The cohesion of the structure is relatively high. Comparatively, Expandable Graphite (EG) is a typical example of intumescent flame retardant that follows a mechanical process. Insertion compounds are contained between the graphite layers and upon heating EG expands: the intercalation compound quickly decomposes into gaseous products, thereby exposing the graphite flakes which then form an entangled network of worm-like structures on the surface of the loaded material. This network acts as a protective layer that expands under the rapid sublimation of molecules in the polymeric matrix [21, 22]. It should be noted that the cohesion of the structure is high enough to provide the protection of interest but it is not strong to resist the fluid flow or other erosion forces. The structure difference between AP and EG could lead to a different mass transfer of gaseous fuel to the flame. An image of the AP and EG residues after combustion is provided as supplementary material to show the difference in their structure.

To investigate the influence of different flame retardants on flame spread at both normal and microgravity, this paper investigates the consequences of AP and EG addition to standard samples. Many of the results depend on the particular configuration. That being said, the axisymmetric configuration gives access to a relatively simple topology of the flow field and the opposed flow feature leads to a minimal still relevant interaction between the flame and the condensed phase. As a result, the configuration investigated is believed to offer a fine compromise between applied challenges and fundamental ambitions for the specific study of flame retardants and especially their influence on the condensed phase. Therefore, thin cylindrical samples of LDPE are used as a baseline, to build on the existing literature with uni-directional flame spread. Experiments are then performed on the ground and in parabolic flights to study the extinction limit, the average flame spread rate, and smoke emission in the opposed-flow configuration, under varying oxygen content.

2. Methodology

2.1. Experimental setup

All experiments at normal and micro-gravity are conducted on the Detection of Ignition And Mitigation Onboard for Non-Damaged Spacecrafts (DIAMONDS) rig, extensively detailed in Refs. [23–25]. To conduct microgravity experiments, DIAMONDS is installed aboard Novespace A310 ZeroG aircraft which performs parabolic flights. Each parabola provides 22 seconds of microgravity, with an absolute residual acceleration below $5 \times 10^{-2} \mathrm{g}_0$.

Briefly, DIAMONDS features a cylindrical combustion chamber with an internal diameter of 190mm where a laminar flow of controlled oxygen content, pressure, and velocity is established. The ranges of controlled oxygen content, ambient pressure level and flow velocity are 0% to 21% in volume, 50 kPa to 150 kPa, and 0 to 300mm/s, respectively. In the following, the flow velocity and the pressure are set at 150mm/s and 101.3 kPa, respectively, and the oxygen content is investigated from 17 to 21%. The samples studied are LDPE cylinders, potentially loaded with intumescent flame retardants. The samples are 100mm long, with a diameter of 2mm. Unlike previously studied samples [23], they do not feature a metallic core that affects both heat transfer and the integrity of the condensed phase as the flame propagates. The sample, located at the center of the combustion chamber along its axis, is ignited without contact using a hot incandescent Kanthal wire. A 14.2V current flows for 8s in the Kanthal wire as the aircraft enters its parabolic trajectory, regardless of whether ignition happens or not. Since the present study on the flame retardant sample is based on the opposed-flow flame spread, the coil is placed at the upstream end of the samples.

Once the sample is ignited, the flame propagation is recorded by a JAI AT-140CL digital 12-bit tri-CCD camera. This camera, equipped with a telecentric lens, images the incoming light over red, green, and blue 521x1396 pixel^2 CCD arrays with a spatial resolution of 72.6μm at a rate of 39fps. At the back of the sample, uniform backlighting produced by a set of adjustable RGBW LEDs is alternatively set on and off during the images recording. The solid fuel surface can be observed on the backlighted images to investigate the intumescence produced by the different types of flame retardant. In addition, the backlight allows discrimination between smoking and non-smoking conditions through observation of absorption at the flame trailing edge. Besides, a 640x480 VIM 640 G2 ULC Infrared camera with a working spectral range from 8μm to 14μm, a resolution of 86μm, and a frame rate of 30fps has been added along the direction perpendicular to the line-of-sight of the tri-CCD camera. This additional camera measures the infrared energy emitted from the surface of samples through a polished germanium window with a transmission spectrum between 2μm and 14μm. Moreover, a passively athermalized infrared lens is mounted in order to block the infrared signal in a spectral band from 8μm to 12μm.

Observations are carried out 15 to 25 seconds after ignition. This allows the flame to spread away from the

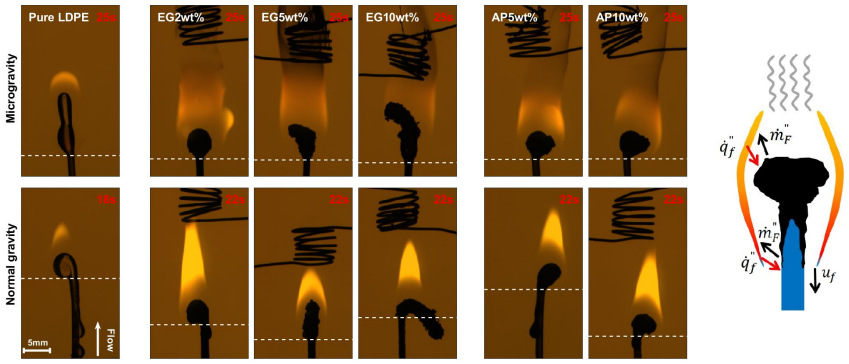

Fig. 1: Backlighted frames imaging opposed-flow flame spread over cylindrical LDPE samples (left) and schematic of the degradation process (right). All observations are carried out at a pressure of 101.3 kPa, under an oxygen content of 21% and a flow velocity of 150 mm/s, to observe the impact of gravity and both AP and EG flame retardants with varying weight contents. The images are taken 15s after ignition, shortly before the end of the flame spread. The time since ignition is indicated in the upper right corner of every frame. The position of the upstream condensed phase deformation is indicated by a dashed line.

igniter and reduce undesired interactions while making sure flame spread is analyzed in the steady microgravity phase of the parabola.

2.2. Samples manufacturing process

LDPE was supplied by Sabic (Netherlands) in the commercial grade Sabic® LDPE 2602X1 00900. EG is the commercial grade ES350F5 from Graphitwerk Kropfmühl (Germany) with an average particle size of 300 µm. Sulfate was used in this grade as an intercalation compound to make graphite bisulfate. APP is the commercial grade of Clariant (Germany) with the brand name Exolit AP422. PER was supplied by Aldrich.
LDPE was blended with flame retardants in a twin-screw extruder. The total loading of flame retardants in LDPE varied from 2 to 10 wt% of EG and at 5 and 10 wt% for APP/PER with the ratio 3:1 (wt/wt) and hereafter called AP. Compounding was performed using HAAKE Rheomix OS PTW 16 twin-screw extruder. The extruder is a co-rotating intermeshing twin screw with a barrel length of 400 mm and a screw diameter of 16 mm (L/D = 25) with 10 zones. LDPE and flame retardants were incorporated using two gravimetric side feeders into the extruder. The polymer flow rate is fixed to extrude about 500 g/h with a screw speed of 300 rpm.
Since the purpose of the present study is to observe the influence of flame retardant on flame spread from 17 to 21% oxygen content, the flame retardant loading needs to be adjusted to adapt to the general requirements. Here, flame retardants are incorporated into the LDPE solid phase, with proportions of 2wt%, 5wt%, and 10wt% for EG, and 5wt%, 10wt% for AP. To provide a baseline, pure LDPE samples are also investigated.

3. Results and discussion

3.1. Initial observation

Figure 1 displays backlighted observations of samples at normal and micro-gravity, with various flame retardant contents, at a set oxygen content of 21%.

The expansion linked to the intumescent processes is clearly visible in microgravity, as illustrated in Fig. 1. AP loaded samples feature a globally spherical shape in the pyrolyzing region with a size independent of the loading. Yet, this region is larger in microgravity than at normal gravity. In contrast, the intumescent region of EG-loaded samples increases in size with the EG loading, moving from a spherical shape towards a more cylindrical structure. As the expanded carbon layers accumulate, the intumescent region severely bents, and even drops under its own weight at normal gravity, affecting the protection of the unburnt upstream part. Ahead of the intumescent region, dripping is also recorded at normal gravity and increases as the content of flame retardant decreases.

Over pure LDPE samples, a strong dripping process is observed. At normal gravity, the intense dripping carries most of the molten fuel away, leading to a short flame length. The dripping occurs due to the effect of gravitational force on the accumulated molten droplet generated by the pyrolysis process of LDPE. It has been observed that the dripping also occurs with a sample at low flame retardant loading (e.g. EG2wt% and AP5wt%), but as the loading continues to increase, the dripping is reduced. In microgravity, a complex motion of twin droplets is observed ahead of the flame. The droplets regularly merge and separate as the flame spreads, with no correlation to the residual gravity, evidencing competing flow mechanisms in the molten phase.

Over flame retardant-loaded samples, the luminosity of the flame does not significantly change at a set gravity level, in spite of the severe modifications in the condensed phase with the increased intumescent load. However, as the flame retardant load increases, the flame seems to be more stable, with weaker flickering. At normal gravity, the flame is bright and stretched, while it is wider and less luminous in mi-

crogravity. This points to an increased residence time and a lower local soot temperature, which promotes quenching at the flame trailing edge. A dark trail of smoke is systematically observed over flame retardant-loaded samples in microgravity, though it was not reported over the pure LDPE samples. As such, EG and AP seem to promote quenching, which results in increased atmospheric contamination. This illustrates the need for systematic characterization of flame retardant performance in the absence of buoyant flows, as increased smoke production questions their efficiency.

A schematic is shown in Fig. 1 to further analyze the mechanism of flame retardants affecting the flame spread. The heat flux, $\dot{q}''_f$, from the flame to the sample surface is transferred to the unburned zone at the leading edge of the flame, and the addition of flame retardants slows down the local pyrolysis rate $\dot{m}''_F$ of the solid fuel. This influences the overall pyrolysis rate $\dot{m}_F$, therefore the flame spread rate, u_f, as shown by Eq. (1), and potentially stops the flame spreading. In addition, the intumescent region also blocks a part of the heat, $\dot{q}''_f$, which weakens the pyrolysis process and contributes to the mitigation of the flame spread. The gaseous fuel supplied by the pyrolysis needs to flow through the intumescent region to reach the trailing edge of the flame, and this process tends to increase the residence time, which favors soot production in the flame, thus increasing the hazard of smoke emission.

3.2. Extinction limits

Flame propagation and self-extinction are investigated first and reported in Fig. 2. Since the igniter provides a large external heat flux in the first few seconds of each experiment, a visible flame appears systematically. During the observation period, if combustion is not self-sustained, the flame gets smaller and less luminous until it eventually quenches at its leading edge, then releasing a significant amount of unburnt pyrolysis gases and possibly soot particles which are visible through backlight attenuation. Such a situation is regarded as extinction [26]. The infrared camera provides additional clues regarding the surface temperature evolution. If combustion is sustained at the flame leading edge and the flame spreads, a pyrolysis region of uniform and stable temperature is recorded. In an extinction situation, the infrared signal gradually drops, starting from the upstream preheating region, as heat loss mechanisms dominate in the condensed phase. The infrared signal collects quantitative information ahead of the potential visible flame extinction, thus increasing confidence in the discrimination of spread and extinction situations within the limited observation period.

Under normal gravity conditions, flame retardants have a noticeable impact on flame extinction. Under the pressure and flow velocity conditions studied, the LOI is raised from 18% for the pure LDPE sample to 19% for both EG- and AP-loaded samples, and is even increased to 21% for 10wt% AP-loaded samples. Increasing the EG load does not show any significant effect on flame extinction. This is interpreted as a consequence of the increase in intumescence volume, which triggers subsequent bending and falling off of the expanded carbon layer under the influence of gravity. As this protective thermal insulation layer is removed, the virgin fuel is exposed to the flame heat flux, which promotes pyrolysis and cancels the benefits of increased EG loading. On the other hand, the increase in AP loading results in a higher LOI since the more compact intumescent volume never detaches from the fuel surface, thus retaining its protective function. Unlike normal gravity observations, no shift in LOI was reported in microgravity for both flame retardants regardless of the loading. The flames could spread at 18% oxygen content, the LOI for the pure LDPE sample, in spite of the visible intumescence (see Fig. 1). As such, the intumescence does not improve on the ex-

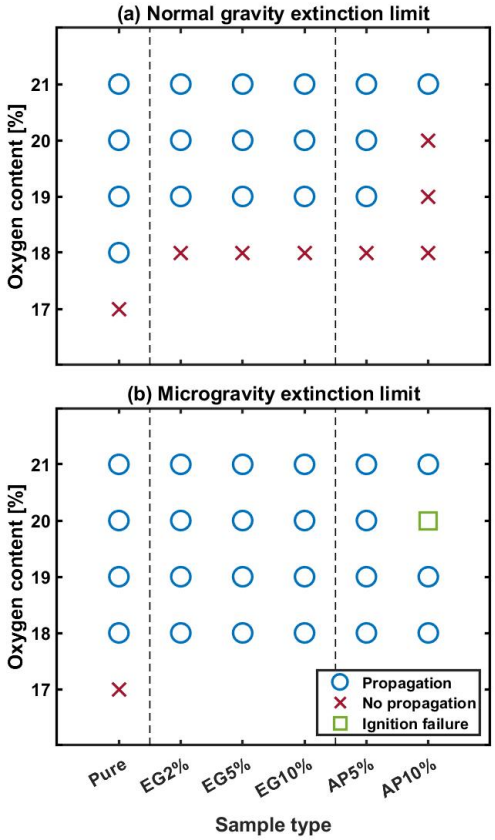

Fig. 2: Effect of oxygen content on flame spread and extinction over LDPE samples loaded with various flame retardant contents under (a) normal and (b) micro-gravity conditions. The noticeable impact of flame retardants on extinction at normal gravity disappears in microgravity.

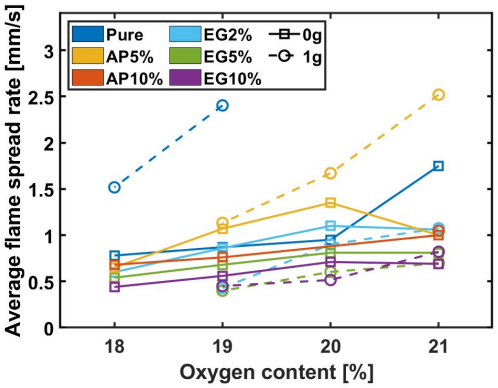

Fig. 3: Effect of oxygen content on average flame spread rate at normal and micro-gravity. Each color corresponds to a type of sample and two different markers represent two different gravity levels. Flame retardants hinder the spread of flame at both normal and micro-gravity. The associated uncertainties extracted from the measurement of the pyrolysis position and the frame rate of the camera are lower than 2.5% of the average flame spread rate (see the supplementary material for the set of estimated values).

tinction limit of the studied material under the investigated conditions. This lack of correspondence between normal and micro-gravity observations is particularly problematic as present spacecraft material flammability tests performed on the ground rely on self-extinction criteria [27]. A possible explanation is that the intumescent matrix acts as a porous media in the condensed phase, driving the molten fuel towards the flame through capillarity. This mechanism is shrouded by dripping at normal gravity but dominates the viscous flow in microgravity. In addition, the absence of natural convection prevents blow off at the flame leading edge from the increased buoyancy induced air velocity, as the Damkohler number is increased in microgravity [28].

3.3. Average flame spread rate

The steadiness of spread rate for a given sample and flow condition is evaluated based on the steadiness of the flame length, of the droplet volume, and of the velocity of the flame front position over the period of interest [25]. In all studied conditions, the flame length and the droplet volume continuously increase, so no condition can be considered as a steady flame spread. An average flame spread rate is then estimated by averaging the displacement of the pyrolysis front over the 10s of observation, with the pyrolysis front being defined as the upstream deformation position of the condensed phase (see Fig. 1).

The average flame spread rate at normal gravity and microgravity is plotted as a function of the oxygen content in Fig. 3. It should be pointed out that the pure LDPE results at normal gravity under 20 and 21% oxygen content are not reported, because the sample was fully consumed before the end of the observation period. Still, the average flame spread rate for these two conditions can be considered higher than all the other ones. Overall, the average flame spread rate increases with the oxygen content, for all flame retardant types and loads, and under both normal and micro-gravity conditions. This is expected as the increased flame temperature enhances the heat transfers to the sample surface.

At normal gravity and at a set oxygen content, the average flame spread rate decreases when increasing EG and AP flame retardants loads. In the absence of flame retardant in microgravity, the samples have a tendency to release two droplets upstream of the flame (see Fig. 1 bottom left), which slows down the propagation as the molten fuel cools down upstream of the flame, thus increasing heat losses. As flame retardant is added, this process is not observed anymore, which increases the flame spread rate for the lowest flame retardant loadings (EG2wt% and AP5wt%) compared to the pure LDPE situation. Yet, as the loading is further increased, a reduction in spread rate is observed. Comparing the amplitude of flame spread rate, higher flame retardant loading is required in microgravity to reduce the spread rate to an extent similar to normal gravity observations, where the slowest spread rates are reported. It is interesting that the EG-loaded sample tends to provide a higher flame spread rate in microgravity than at normal gravity. The main reason may be associated with the dripping effect. At normal gravity, the increase in EG loading is correlated with a reduced dripping rate. Different effects may contribute to this trend. Among others, the enhanced rugosity associated with the intumescent material, and more specifically the worms formed with EG addition (see the supplementary material), increases the adherence of the molten droplet at the contact location. As a result, the deceleration of the flame spread with EG loading is significant at normal gravity. In addition, the above trend leads to a certain collapse of the molten droplet formation phenomenology for normal and micro-gravity conditions. However, at normal gravity, the heat of the flame is transferred downstream of the flame especially by the buoyant flow, which reduces the heat transferred upstream, therefore weakening the pyrolysis process. The latest trend can then explain the lower spread rate at normal gravity as compared to that in microgravity as EG loading significantly affects the spread.

Overall, the EG-loaded samples spread more slowly than the AP-loaded samples for the same flame retardant load, under both normal and micro-gravity conditions.

3.4. Smoke emission

In spreading situation where the flame does not quench at the leading edge, local extinction can still take place at the trailing edge, leading to contamination of the surrounding atmosphere. The tendency of the flame to emit smoke can be simply evaluated us-

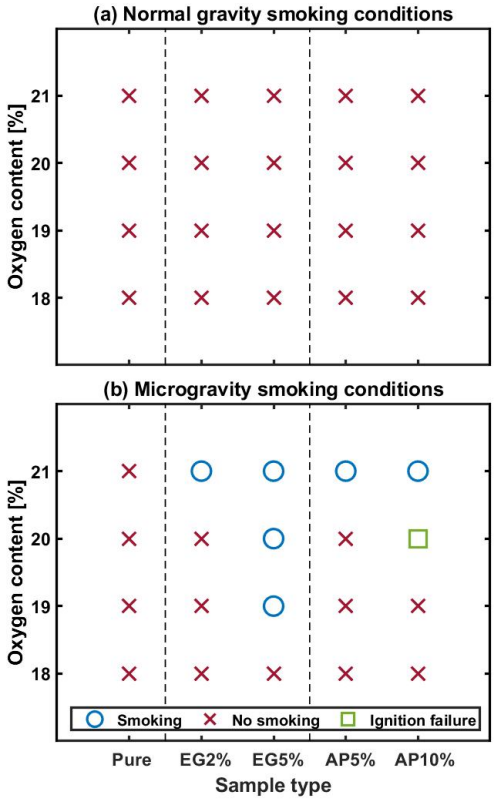

Fig. 4: Effect of oxygen content on smoke emission over LDPE samples loaded with various flame retardant contents under (a) normal and (b) micro-gravity conditions. Flame retardants promote smoke emission in microgravity.

ing the backlighted frames, and results are reported in Fig. 4. Smoke-emitting conditions are defined as spreading situations where a continuous flow of broadband absorbing soot particles is reported at the flame trailing edge. On the contrary, smoke-free conditions are defined as spreading situations where the closed-tip flame does not display detectable absorption at the trailing edge (see both Pure LDPE conditions in Fig 1 for instance). It is worth reporting that the flame spread over the EG 10wt% samples is too slow to discriminate the smoking condition, since the flame trailing edge is still intertwined with the igniter.

At both normal and micro-gravity, no smoke emission was observed over pure LDPE in the studied range of oxygen contents. At normal gravity, no smoke emission is also reported for all flame retardant-loaded samples, over the range of oxygen contents studied. It should be pointed out that results are affected by significant dripping, which can reduce the fuel supply to the flame, thereby reducing soot production. Besides, it is also worth mentioning that the decrease in soot residence time within buoyant flames also reduces the radiative heat losses, leading to flame temperatures at the trailing edge high enough to support complete soot oxidation.

Under microgravity conditions, flame retardant-loaded samples show a consistent tendency to emit smoke at an oxygen content of 21% for all flame retardant types and loading. In addition, smoke emission is also observed at an oxygen content as low as 19% for EG-loaded samples of 5 wt%. But, since the nature of EG and AP intumescence is different, the mechanisms leading to smoke emission are different. EG expansion creates graphite worms through rapid sublimation. As such, it promotes the production of carbonaceous elements which can be released in the flame. Combined with the increase in residence time and hence radiative losses in microgravity, this promotes smoke release. In addition, higher EG loading leads to an increase in carbon particle production and thus also increases the possibility of smoke emission. AP expansion, on the other hand, is driven by a carbonation mechanism that also promotes smoke emission. When the AP loading increases, the amount of char promoters also increases, thus strengthening the carbonation mechanism. As a result, the smoking also increases with AP loading. Comparing both flame retardants, the increase in EG loading causes the smoke emission transition to occur at lower oxygen content conditions, while the increase in AP loading has relatively a weaker impact on smoke emission. This is attributed to the different intumescent mechanisms, affecting the pyrolysis processes differently as oxygen content is increased. The gaseous fuel generated from pyrolysis flows through the intumescent region up to the trailing edge. This tends to increase the residence time, favoring soot production, which increases the hazard of smoke emission. As compared to the AP-loaded sample, the EG-loaded one produces a larger intumescent region at similar loading, which leads also to a longer residence time, further promoting the smoke emission. In addition, the cohesion of the EG residue structure is lower than that of the AP residue after combustion. As a result, it can be anticipated that the carbonaceous matter is released at a higher rate from the EG-loaded sample, which also promotes the smoke emission.

Smoke emission is heavily influenced by oxygen content in microgravity, as the flames spreading over all flame retardant-loaded samples transition from non-smoking to smoking when the oxygen content is increased. Oxygen content has a mixed effect on smoke emission. Higher oxygen content provides higher stoichiometric flame temperature and a higher soot oxidation rate [29], which should block smoke emission. But from the results of the previous section, it also appears that the flame spread rate,and consequently the pyrolysis rate, increases with oxygen content, which facilitates smoke production [12]. And the pyrolysis rate is determined as:

$$\dot{m}_F = \rho_{pe} \cdot \pi \cdot r_s^2 \cdot u_f \tag{1}$$

where ρ_{pe} is the density of LDPE, r_s is the cylinder radius and u_f is the spread rate.

Table 1: Flame spread rate exponent β for different samples in microgravity

Pure	EG2%	EG5%	EG10%	AP5%	AP10%
4.84 ± 1.76	3.84 ± 1.16	2.73 ± 0.67	3.11 ± 0.79	3.05 ± 2.35	2.53 ± 0.17

To further investigate the role of oxygen content, the relationship between pyrolysis mass flow rate $\dot{m_F}$ and oxygen content x_{O_2} is quantified, following Guibaud et al. [30]. The power law relating pyrolysis mass flow rate to oxygen content is extracted from a least square optimization using logarithmic transform to identify the parameter β, as shown in Eq. (2).

$$\dot{m}_F = C\, x_{O_2,\infty}^{\beta} \tag{2}$$

where C is a constant.
The value of β is then contrasted to a previous investigation by Glassman and Yaccarino at normal gravity [31]. The authors investigated the effect of oxygen content on a coflow diffusion flame at atmospheric pressure, and reported the variation of critical ethylene fuel flow rate $\dot{m}_F^c$ to sustain quenching conditions at the flame tip. Based on the variation of this critical value in the oxygen content range of the present experiment, a critical mass flow rate can be obtained as:

$$\dot{m}_F^c = C\, x_{O_2,\infty}^{0.82\pm0.14} \tag{3}$$

Any variation above this critical value fosters smoke emission, while any variation below hampers smoke emission. With the present configuration, the fuel is made of a similar chemical structure at the molecular level (polyethylene). Still, it is solid and the fuel pyrolysis rate is especially a function of the oxygen content, therefore cannot be freely adjusted. To understand whether a variation in oxygen content and the subsequent variation in fuel mass flow rate can trigger the release of smoke, a method similar to that of Glassman and Yaccarino is also applied to the present results in microgravity. The values of β extracted for the different sample types (reported in Tab. 1) are contrasted with the critical variation reported by Glassman and Yaccarino. All values for β are higher than the critical fuel flow rate variation of Eq. (3), so it can be concluded that the pyrolysis mass flow rate of all samples in microgravity increases faster than the critical mass flow rate required to sustain quenching at the flame trailing edge as the oxygen content increases. This means that the increase in pyrolysis mass flow rate with oxygen can be sufficient to justify a transition from non-smoking to smoking conditions. In addition, in the present case and as stated previously, the smoke release is also promoted by the effect of flame retardants on pyrolysis. Consequently, if high flame retardants loadings can further reduce flame spread rate until the increase in pyrolysis rate drops below its critical value, the transition from non-smoking to smoking still needs to be verified.

4. Conclusion

LDPE samples loaded with two types of intumescent flame retardants, EG and AP, were ignited at varying levels of oxygen content at normal and microgravity, to analyze the associated extinction limits, flame spread rates, and smoke emissions. The results show strong differences between microgravity and normal gravity conditions, which call for cautious integration of flame retardants in the scope of space exploration. The extinction limit increases with flame retardants loading at normal gravity, but this effect is not reported in microgravity. At normal gravity, an increased flame retardant load inhibits flame spread, this effect is also observed, though less pronounced, when assessing the average spread rate in microgravity. Under the same ambient conditions and the same loading, EG-loaded samples show a reduced flame spread rate compared to AP-loaded samples. To confirm that these results stand once the flame spreads steadily, similar long-duration experiments are required. Though flame retardants enhance fire safety in microgravity by lowering the flame spread rate, they also facilitate smoke emission to an extent that is not reported at normal gravity. The enhanced propensity to emit smoke is especially noticeable over the EG-loaded sample in spite of the lower flame spread rate, because the intumescence production mechanism readily contributes to soot formation in the absence of gravity. Globally, it is observed that the combustion characteristics of samples loaded with flame retardants in microgravity are different from those at normal gravity, stressing the need for additional experimental observations prior to their adoption in spacecraft design.

Acknowledgments

The authors feel grateful to the Centre National d'Etudes Spatiales (CNES) for its financial support under Contract No. 130615.

Supplementary material

An image of AP and EG residue after combustion and the data of average flame spread rates and their uncertainties are provided as supplementary material.

References

[1] National Research Council, Recapturing a Future for Space Exploration: Life and Physical Sciences Research for a New Era, The National Academies Press, Washington, DC, 2011.

[2] O. Fujita, Solid combustion research in microgravity as a basis of fire safety in space, Proc. Combust. Inst. 35 (3) (2015) 2487–2502.

[3] G. Jomaas, J. L. Torero, C. Eigenbrod, J. Niehaus, S. L. Olson, P. V. Ferkul, G. Legros, A. C. Fernandez-Pello, A. J. Cowlard, S. Rouvreau, et al., Fire safety in space–beyond flammability testing of small samples, Acta Astronautica 109 (2015) 208–216.

[4] S. Olson, M. Johnston, J. T'ien, Flammability Aspects of a Cotton-Fiberglass Fabric in Opposed and Concurrent Airflow in Microgravity, American Society for Gravitational and Space Research, 2012.

[5] S. Link, X. Huang, C. Fernandez-Pello, S. Olson, P. Ferkul, The effect of gravity on flame spread over pmma cylinders, Scientific reports 8 (1) (2018) 1–9.

[6] A. Guibaud, J.-M. Citerne, J.-L. Consalvi, J. L. Torero, O. Fujita, M. Kikuchi, P. V. Ferkul, N. Smirnov, G. Jomaas, B. Toth, S. Rouvreau, G. Legros, Accessing the soot-related radiative heat feedback in a flame spreading in microgravity: optical designs and associated limitations, Proc. Combust. Inst. 38 (3) (2021) 4805–4814.

[7] Y. Nakamura, T. Kashiwagi, S. Olson, K. Nishizawa, O. Fujita, K. Ito, Two-sided ignition of a thin pmma sheet in microgravity, Proc. Combust. Inst. 30 (2) (2005) 2319–2325.

[8] M. A. Delichatsios, R. A. Altenkirch, M. F. Bundy, S. Bhattacharjee, L. Tang, K. Sacksteder, Creeping flame spread along fuel cylinders in forced and natural flows and microgravity, Proc. Combust. Inst. 28 (2) (2000) 2835–2842.

[9] O. Fujita, T. Kyono, Y. Kido, H. Ito, Y. Nakamura, Ignition of electrical wire insulation with short-term excess electric current in microgravity, Proc. Combust. Inst. 33 (2) (2011) 2617–2623.

[10] S. Takahashi, H. Ito, Y. Nakamura, O. Fujita, Extinction limits of spreading flames over wires in microgravity, Combustion and flame 160 (9) (2013) 1900–1902.

[11] P. S. Greenberg, K. R. Sacksteder, T. Kashiwagi, Wire insulation flammability experiment: Usml-1 one year post mission summary, Joint Launch and One Year Science Review of USML-1 and USMP-7 with the Microgravity Measurement Group 2 (1994).

[12] A. Guibaud, J.-M. Citerne, J.-L. Consalvi, G. Legros, On the effects of opposed flow conditions on non-buoyant flames spreading over polyethylene-coated wires–part i: Spread rate and soot production, Combustion and Flame 221 (2020) 530–543.

[13] S. Garber, J. Linenger, Fire and controversy january 12-may 24, NASA History Program Office (1997).

[14] E. Orndoff, Flame retardant fibers for human space exploration-past, present, and future, Dornbirn Man-Made Fibers Congress (2017).

[15] S. Takahashi, M. A. F. bin Borhan, K. Terashima, A. Hosogai, Y. Kobayashi, Flammability limit of thin flame retardant materials in microgravity environments, Proc. Combust. Inst. 37 (3) (2019) 4257–4265.

[16] S. Takahashi, K. Terashima, M. A. F. bin Borhan, Y. Kobayashi, Relationship between blow-off behavior and limiting oxygen concentration in microgravity environments of flame retardant materials, Fire Technology 56 (1) (2020) 169–183.

[17] G. Fohlen, J. Parker, S. Riccitiello, P. Sawko, Intumescence: an in situ approach to thermal protection, WESRAC-Fireproofing and Safety Symposium (1972).

[18] D. A. Kourtides, Flame-retardant composite materials, Vol. 3109, Technology 2000: Proceedings of a Conference, 1991.

[19] J. Alongi, Z. Han, S. Bourbigot, Intumescence: Tradition versus novelty. a comprehensive review, Progress in Polymer Science 51 (2015) 28–73.

[20] S. Bourbigot, M. Le Bras, R. Delobel, Carbonization mechanisms resulting from intumescence association with the ammonium polyphosphate-pentaerythritol fire retardant system, Carbon 31 (8) (1993) 1219–1230.

[21] S. Bourbigot, J. Sarazin, T. Bensabath, F. Samyn, M. Jimenez, Intumescent polypropylene: reaction to fire and mechanistic aspects, Fire Safety Journal 105 (2019) 261–269.

[22] T. Bensabath, J. Sarazin, M. Jimenez, F. Samyn, S. Bourbigot, Intumescent polypropylene: Interactions between physical and chemical expansion, Fire and Materials 45 (3) (2021) 387–395.

[23] J.-M. Citerne, H. Dutilleul, K. Kizawa, M. Nagachi, O. Fujita, M. Kikuchi, G. Jomaas, S. Rouvreau, J. L. Torero, G. Legros, Fire safety in space–investigating flame spread interaction over wires, Acta Astronautica 126 (2016) 500–509.

[24] A. Guibaud, J. Citerne, J. Orlac'h, O. Fujita, J.-L. Consalvi, J. Torero, G. Legros, Broadband modulated absorption/emission technique to probe sooting flames: Implementation, validation, and limitations, Proc. Combust. Inst. 37 (3) (2019) 3959–3966.

[25] A. Guibaud, J.-M. Citerne, J.-L. Consalvi, O. Fujita, J. Torero, G. Legros, Experimental evaluation of flame radiative feedback: methodology and application to opposed flame spread over coated wires in microgravity, Fire Technology 56 (1) (2020) 185–207.

[26] M. Nagachi, J.-M. Citerne, H. Dutilleul, A. Guibaud, G. Jomaas, G. Legros, N. Hashimoto, O. Fujita, Effect of ambient pressure on the extinction limit for opposed flame spread over an electrical wire in microgravity, Proc. Combust. Inst. 38 (3) (2021) 4767–4774.

[27] D. Mulville, Flammability, odor, offgassing, and compatibility requirements and test procedures for materials in environments that support combustion, Tech. rep., NASA-STD-6001 (1998).

[28] M. C. Johnston, S. James, D. E. Muff, X. Zhao, S. L. Olson, P. V. Ferkul, Self induced buoyant blow off in upward flame spread on thin solid fuels, Fire safety journal 71 (2015) 279–286.

[29] J.-L. Consalvi, A. Guibaud, A. Coimbra, J.-M. Citerne, G. Legros, Effects of oxygen depletion on soot production, emission and radiative heat transfer in opposed-flow flame spreading over insulated wire in microgravity, Combustion and Flame 230 (2021) 111447.

[30] A. Guibaud, J.-M. Citerne, J.-L. Consalvi, G. Legros, On the effects of opposed flow conditions on non-buoyant flames spreading over polyethylene-coated wires–part ii: Soot oxidation quenching and smoke release, Combustion and Flame 221 (2020) 544–551.

[31] I. Glassman, P. Yaccarino, The effect of oxygen concentration on sooting diffusion flames, Combustion Science and Technology 24 (3-4) (1980) 107–114.

Figure 1

Click here to access/download;Figure;fig1.jpg

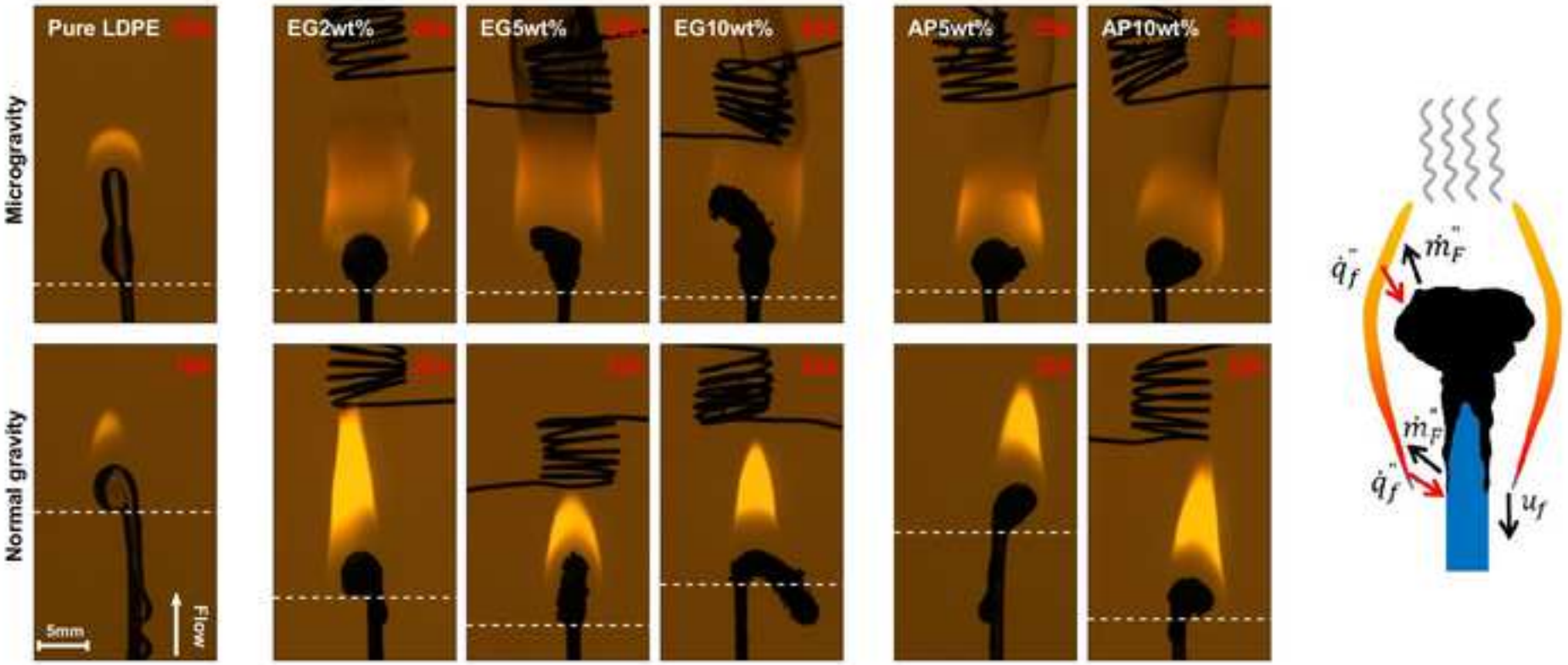

Figure 2

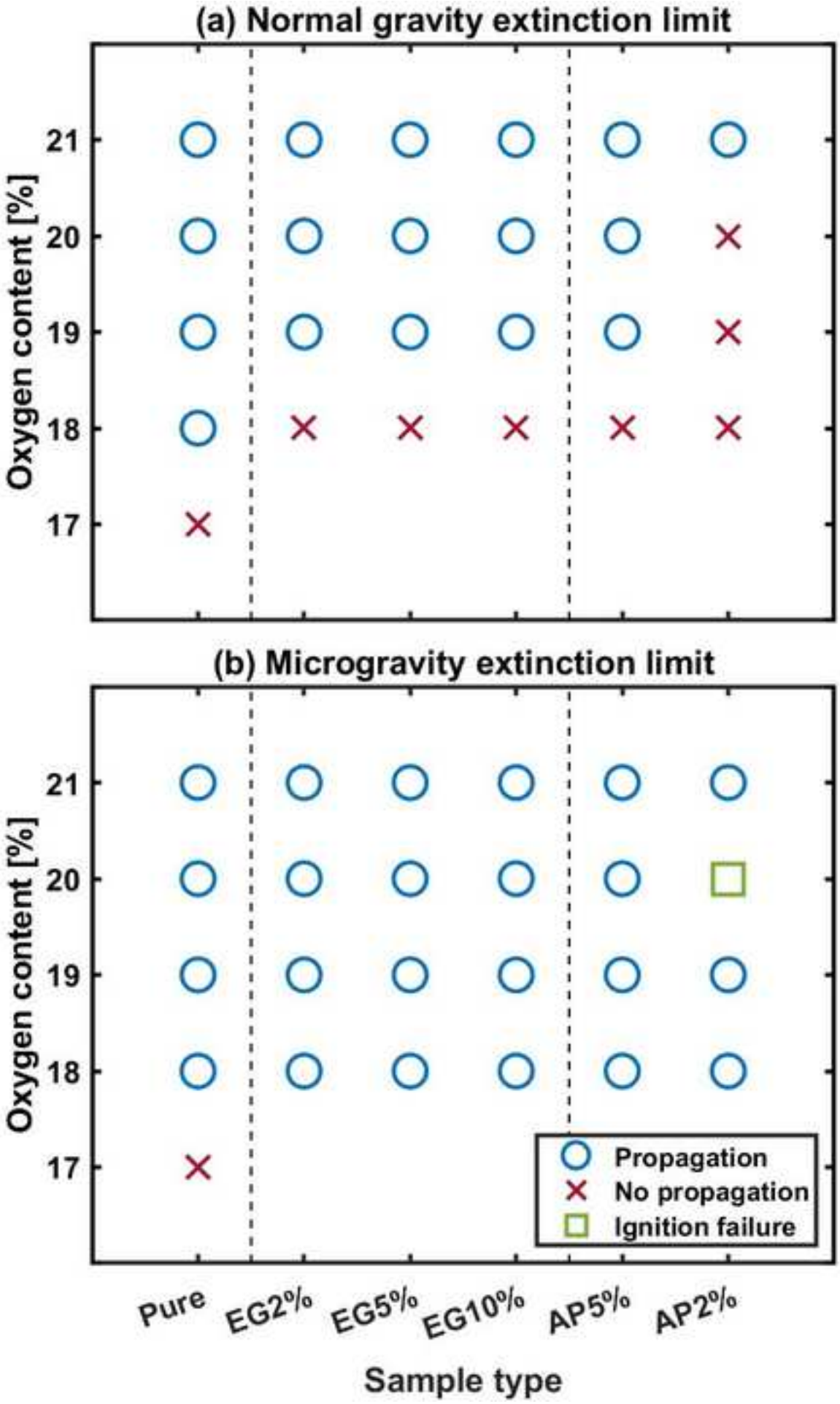

Figure 3

Click here to access/download;Figure;fig3.jpg

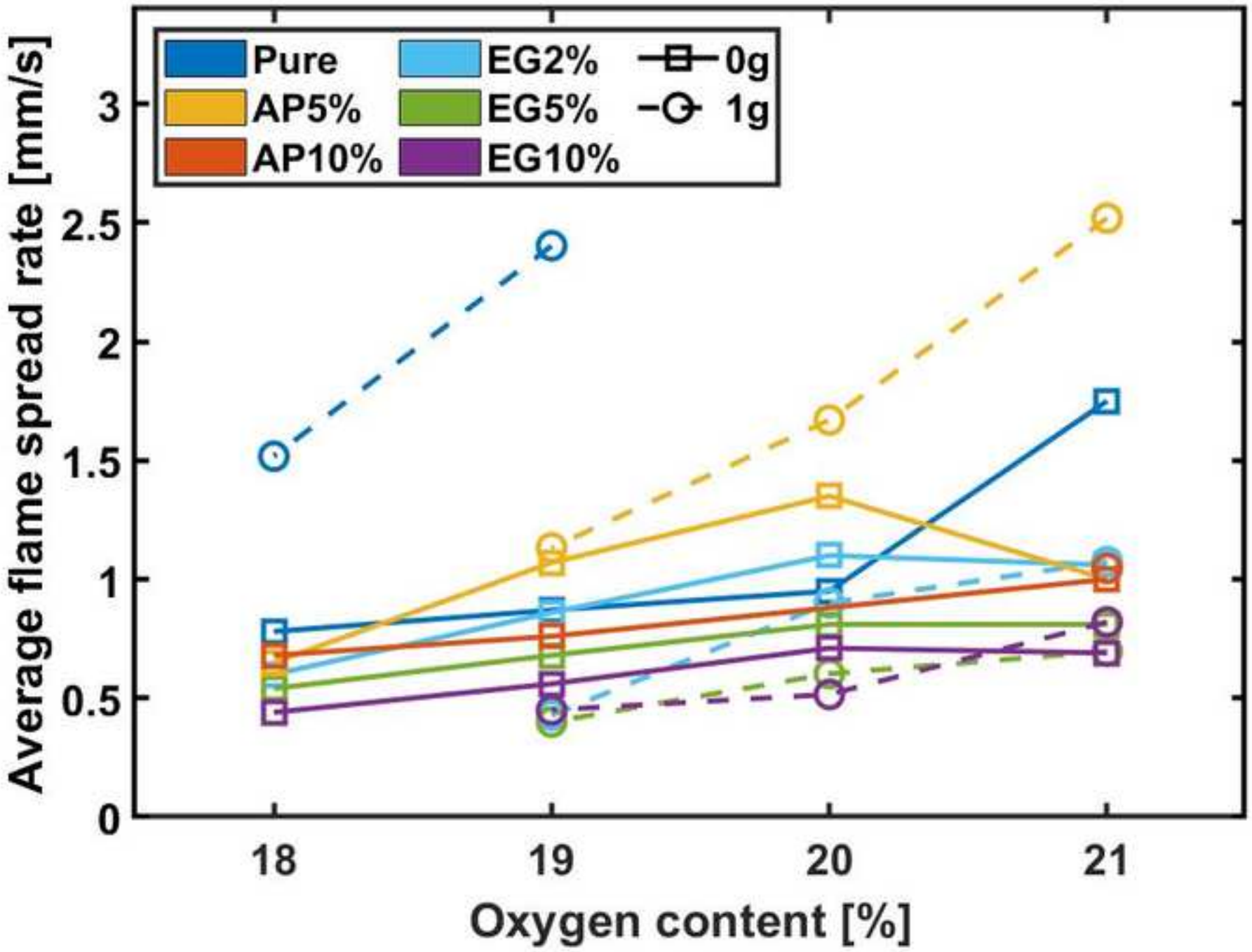

Figure 4